

# Comparison of Several Re-entry Vehicle Base Pressure Correlations

E.J. Kawecki\*

General Electric Company, Philadelphia, Pa.

Some improved re-entry vehicle base pressure correlations for both laminar and turbulent supersonic flows are presented and compared to the appropriate, widely used correlations. The overall prediction accuracy and sensitivity of these correlations are evaluated for ground test data and flight data from 12 different vehicles.

## Nomenclature

|                   |   |
|-------------------|---|
| $D$               | = diameter  |
| $h, H$            | = static and stagnation enthalpy  |
| $h_w$             | = wall static enthalpy  |
| $H_\infty$        | = stagnation enthalpy   |
| $M$               | = Mach number   |
| $M_e$             | = Mach number at rear edge of vehicle (all edge properties are at edge of boundary layer) |
| $P_b$             | = base pressure   |
| $P_e$             | = static pressure at rear edge of vehicle   |
| $P_\infty$        | = static pressure   |
| $R_b$             | = base radius   |
| $Re$              | = Reynolds number   |
| $Re_{R_b}$        | = Reynolds number based on base radius  |
| $Re_s$            | = Reynolds number based on total wetted length  |
| $R_N$             | = nose radius   |
| $R_N/R_b$         | = bluntness ratio   |
| $S$               | = wetted length   |
| $\theta_c$        | = cone half-angle   |
| <i>Subscripts</i> |   |
| $b$               | = base  |
| $e$               | = edge of boundary layer at end of vehicle, experimental                                  |
| $p$               | = predicted   |
| $s$               | = wetted length   |
| $w$               | = wall  |
| $\infty$          | = freestream  |

## Introduction

**A** KNOWLEDGE of the near-wake characteristics of hypersonic axisymmetric vehicles is necessary for the prediction of vehicle drag, base heating, and far-wake characteristics.<sup>1,2</sup> Unfortunately, the analytic treatment of this very complex region has met with only limited success, necessitating the use of experimental correlations to characterize the flow. These correlations are not entirely satisfactory, however, and there is a definite need to improve both their utility and accuracy. A currently important correlation and one in need of improvement in both of these areas is the base pressure correlation.

The empirical nature of base pressure correlations results in their having intrinsic limitations and restrictions. Unfortunately, these generally are not apparent from the format of the correlation nor stated explicitly in the document from which the user/reader obtains the correlation. As a result, care must be taken to understand the limitations and

restrictions of each correlation within the framework of the intended application. To do so, however, requires a knowledge of the data scatter and range of vehicles comprising the correlation. This information will allow a determination of whether the correlation is applicable to the particular problem of interest and what is the expected error in the prediction.

This paper will consider the effectiveness of two existing correlations in predicting the base pressure on vehicles similar to those of their respective data bases. This comparison will be performed using additional data from other slender re-entry vehicles similar to those used in forming these correlations. By using this more extensive data base, additional information on the nature of the correlations is obtained, including an overall estimate of their prediction accuracy and the identification of particular situations where a correlation might be expected to give a superior or less accurate prediction of base pressure. In addition to this evaluation, another correlation is proposed and compared to the existing correlations.

## Data Base

The data utilized in this work are summarized in Table 1. Included in this list are flights of the following vehicles: ABC, MK-3, MK-4, MK-12, MTV, Re-Entry F, REX, RVTO, SAMAST, TVX, and WAC. Analysis of these data requires the calculations of freestream and boundary-layer edge properties in order to form the parameters of the various correlations. The method used to calculate the conditions at the edge of the boundary layer for a given vehicle depended on the source of data for the vehicle. For the ground test data, these calculations were performed by Martellucci<sup>3</sup> using the General Electric-VIZAAD<sup>4</sup> program; the flight test data of Ref. 5 were reduced using the Sandia-BLUNTY<sup>6</sup> program; and the remaining flight data, with the exception of vehicle 7, were reduced by Truncellito using the General Electric-ENSBL program.<sup>8</sup> The computation of edge conditions for vehicle 7 was performed with the General Electric Aerodynamic Heating Program (AHP).

In comparing the ground test data to Bulmer's correlation, an estimate of the edge pressure is required. The conical flow solution for sharp vehicles<sup>9</sup> is used for all vehicles having bluntness ratios up to  $R_N/R_b = 0.06$ . No such simple calculation procedure is available for the higher bluntness ratios, although Martellucci<sup>3</sup> presents VIZAAD edge pressure calculations for some of the higher-bluntness-ratio cases. The remaining small amount of higher bluntness data for which the edge conditions were not available was omitted from the Bulmer correlation. In order to generate the parameters used in Bulmer's correlation from his data, the ratio of specific heats was assumed to be 1.4. A comparison of the data so reduced to those given by Bulmer shows good agreement.

The majority of the data used to generate the laminar correlation were derived from ground tests in which the model

Received July 17, 1976; presented as Paper 76-376 at the AIAA 9th Fluid and Plasma Dynamics Conference, San Diego, Calif., July 14-16, 1976; revision received December 6, 1976.

Index categories: LV/M Aerodynamics; LV/M Flight Testing; LV/M Simulation.

\*Test Engineer, LV/M Aerodynamics Reentry & Environmental Systems Division. Member AIAA.

was supported. Care must be taken when using such ground test data, as there is evidence indicating that support systems alter base flow, resulting in an associated change in the base pressure.<sup>10,11</sup> In order to minimize these effects, only drop test data and data from models supported by wires and compression struts were retained. Specifically excluded were data from sting-supported models.

## Results

### Laminar

A display of the laminar data of this work is shown in Fig. 1, where the ordering of these data on  $P_b/P_\infty$  vs  $Re_s$  coordinates is apparent. The dependence on edge or freestream Mach number demonstrated by Martellucci<sup>3</sup> is apparent, and so, to a lesser extent, is the bluntness dependence. By considering the trends so identified, a transformation to new coordinates may be performed which results in a collapse of these data. The result of such a process is shown in Fig. 2, where the data of Fig. 1 are displayed on the new coordinates.

The significant properties of this correlation are its strong dependence on edge Mach number  $M_e$ , the use of freestream static pressure  $P_\infty$  as a reference, and the explicit dependence on bluntness ratio  $R_N/R_b$ . Note that the actual bluntness ratio is not used over the entire bluntness range, but rather the bluntness factor  $R_N/R_b$ . This factor is defined as follows.

$$\left(\frac{R_N}{R_b}\right)^* = \begin{cases} 0.10 & \text{for } R_N/R_b \leq 0.10 \\ R_N/R_b & \text{for } R_N/R_b \geq 0.10 \end{cases}$$

This continuous factor reflects the observed lack of explicit dependence of base pressure on the bluntness ratio, for bluntness ratios less than a 0.1.

Other works have used different correlating parameters, notably  $RE_{R_b}$  in place of  $Re_s$ ,  $P_e$  in place of  $P_\infty$ , and an

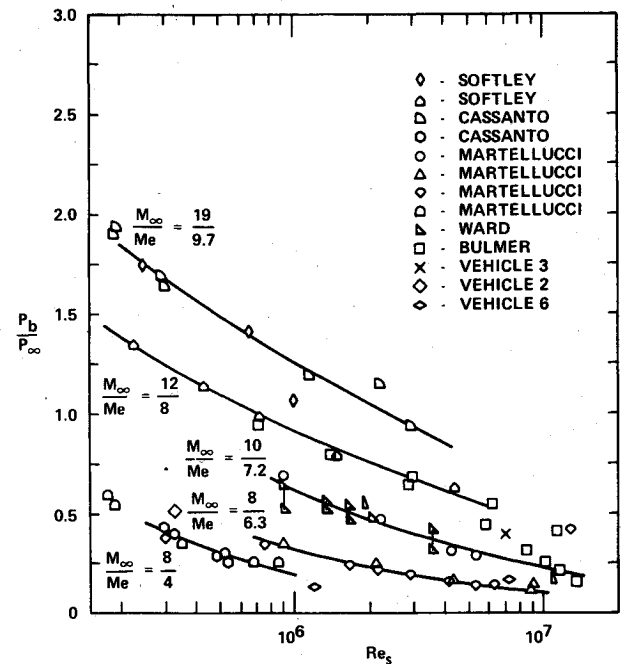


Fig. 1 Laminar base pressure data.

enthalpy factor  $h_w/H_\infty$ . In both the laminar and turbulent cases, the substitution of edge Reynolds number based on base radius  $Re_{R_b}$  for the edge Reynolds number based on wetted length  $Re_s$  results in only a small increase in the data scatter for the data base of the work. This is due primarily to the geometries being nearly the same for all bodies (i.e.,  $4.5 \leq S/R_b \leq 6.4$  for the laminar case, and  $6.1 \leq S/R_b \leq 8.7$  for the turbulent case). This is not the case for the pressure. In the present correlation, the substitution of edge pressure for

Table 1 Data tabulation

| PRESENT SYMBOL | $R_N/R_b$ | $D_b$ (IN.) | $M_e$    | $M_\infty$ | $\theta_e$ (DEG.) | VEHICLE NUMBER | SUPPORT | SOURCE/REFERENCE      |
|----------------|-----------|-------------|----------|------------|-------------------|----------------|---------|-----------------------|
| $\Delta$       | 0         | 5.0         | 9.7      | 19         | 10                |                | F       | GE-CASSANTO/3,7,16,19 |
| $\triangle$    | 0.01      | 4.5         | 9.7      | 19         | 9                 |                | F/W     | GE-SOFTLEY/3, 7,18    |
| $\diamond$     | 0.01      | 4.5         | 8        | 12         | 9                 |                | F/W     | GE-SOFTLEY/3, 7,18    |
| $\circ$        | 0.02      | 6           | 7.2      | 10         | 10                |                | C       | GASL-MART/3,20        |
| $\triangle$    | 0.02      | 6           | 6.3      | 8          | 10                |                | C       | GASL-MART/3,20        |
| $\diamond$     | 0.06      | 6           | 5.7      | 8          | 10                |                | C       | GASL-MART/3,20        |
| $\square$      | 0.15      | 6           | 4        | 8          | 10                |                | C       | GASL-MART/3,20        |
| $\circ$        | 0.3       | 2.0         | 2.4      | 4          | 10                |                | F       | GASL-MART/3,20        |
| $\triangle$    | 0         | 3.8         | 7.2      | 10         | 10                |                | F       | AEDC-WARD/3,17        |
| $\square$      | 0.05      | -           | 9.5-10.5 | 16-20      | 9                 |                | RV      | SANDIA-BULMER/5       |
| $\square$      | 0.30      | -           | -        | -          | 6                 | 1              | RV      |                       |
| $\diamond$     | 0.22      | -           | -        | -          | 7                 | 2              | RV      |                       |
| $\times$       | 0.10      | -           | -        | -          | 6.3               | 3              | RV      |                       |
| $\circ$        | 0.32      | -           | -        | -          | 5.9               | 4              | RV      |                       |
| $\frac{1}{2}+$ | 0.22      | -           | -        | -          | 7                 | 5              | RV      |                       |
| $\diamond$     | 0.04      | -           | -        | -          | 9                 | 6              | RV      |                       |
| $\diamond$     | 0.15      | -           | -        | -          | 5                 | 7              | RV      |                       |
| $\nabla$       | 0.05      | -           | -        | -          | 9                 | 8              | RV      |                       |
| $\oplus$       | 0.06      | -           | -        | -          | 9                 | 9              | RV      |                       |
| $\nabla$       | 0.03      | -           | -        | -          | 8                 | 10             | RV      |                       |
| $\circ$        | 0.007     | -           | -        | -          | 5                 | 11             | RV      |                       |
| $\triangle$    | 0.016     | -           | -        | -          | 10                | 12             | RV      |                       |
| $\circ$        | 0.016     | -           | -        | -          | 10                | 13             | RV      |                       |

| KEY |  |
|-----|--|
| F   | FREE FLIGHT (DROP)                     |
| F/W | FREE FLIGHT WITH INITIAL WIRE SUPPORTS |
| C   | COMPRESSION STRUT                      |
| RV  | RE-ENTRY VEHICLE                       |

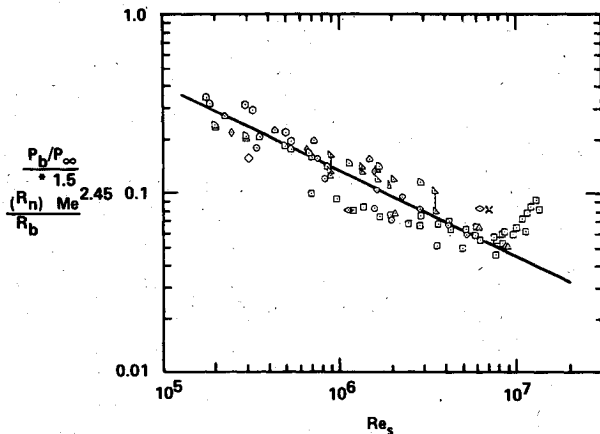


Fig. 2 Laminar base pressure correlation of this work.

freestream static pressure results in a major increase in the scatter. The use of edge pressure has led to reasonable correlations when other correlating parameters were chosen.<sup>5,12</sup>

Bulmer found that incorporation of the enthalpy factor  $h_w/H_\infty$  in the form proposed by Reeves and Buss<sup>13</sup> was required to correlate his data. No such dependence was noted in the coordinates of this work. Consequently, this factor was not included in the present correlating parameter.

It is interesting to note that within each group of data the trend is to parallel the correlation line (Fig. 2). An exception to this trend is the flight data of Bulmer, where the data follow the trend line for Reynolds numbers up to  $10^7$  but after this depart sharply from the correlation trend. This departure may be due to a laminar phenomenon not accounted for in the correlation, or it may be due to a departure from laminar flow in the data. Bulmer does state that all of the data presented are laminar. Additional high Reynolds number data are required to determine if the trend is more than a peculiarity of this one data group.

In the correlation shown in Fig. 1, many geometrical and aerodynamic parameters are not accounted for explicitly. Among them are roll rate, mass addition, angle of attack, and roughness. The absence of an explicit dependence on these parameters does not mean that their effects are entirely unaccounted for. By evaluating the correlation parameters at the rear edge of the vehicle, the effects of mass addition and angles of attack are, to some extent, included implicitly in the correlation through their influence on the conditions at the rear edge of the vehicle. This is not equivalent to including these parameters explicitly in the correlation.

#### Comparison of Base Pressure Correlations

A comparison of the present laminar correlation to those of Bulmer<sup>5</sup> and Cassanto<sup>12</sup> is described in this section. To facilitate this comparison, Bulmer's correlation is shown in Fig. 3. Cassanto's correlation is in the form of an algorithm and therefore is not listed. The complete algorithm is available in the literature.<sup>4,12</sup>

In order to avoid masking the capabilities and shortcomings of each correlation in the particular format of that correlation, each is used to make a prediction of base pressure at test conditions corresponding to an experiment where the base pressure has been measured. This prediction then is compared to the measured base pressure. The results of this comparison are illustrated in Fig. 4, where the ratio of the predicted  $p$  to the experimentally determined  $e$  base pressures are shown for the respective correlations. The scatter in the Bulmer correlation is seen to be only slightly greater than that of this work. It also is evident that both the Cassanto and Bulmer correlations have a bias in their respective predictions of base pressure (i.e., the Cassanto correlation overpredicts the base pressure, whereas the Bulmer correlation un-

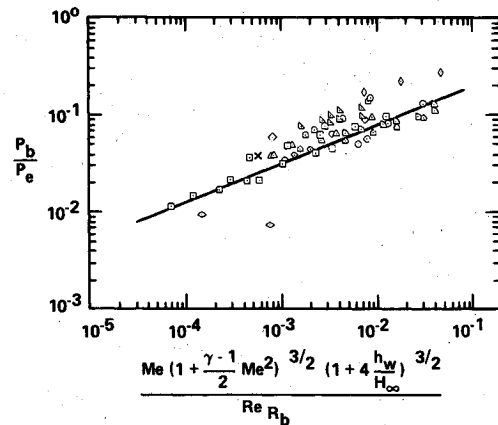


Fig. 3 Bulmer-Sandia laminar base pressure correlation.

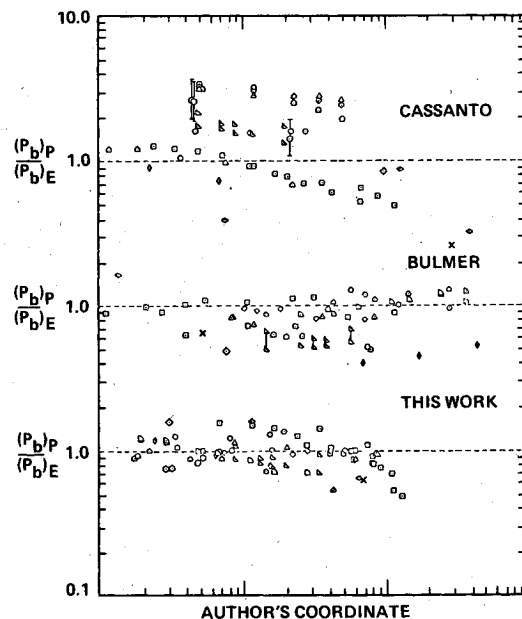


Fig. 4 Comparison of the predicted and experimental laminar base pressures.

derpredicts it for this particular data base). A shift in the level of either correlation would correct this particular problem. It would not affect the data scatter, which is a property of the coordinates and not the particular curve chosen as the correlation. With the present correlation, the largest discrepancy between the predicted and measured base pressures occurs with the high Reynolds number data of Bulmer. An interesting point is that Cassanto's correlation also shows the same tendency for this data group.

The magnitude of the scatter in Fig. 4 provides an estimate of expected accuracy of the correlations when used as predictive tools. As is apparent, the majority of the predictions fall within a  $\pm 50\%$  band about the data. For similar vehicles, it then is reasonable to expect these correlations to provide a base pressure estimate within  $\pm 50\%$  of the actual base pressures.

#### Turbulent Correlations

The laminar correlations of Bulmer, Cassanto, and this work display strong dependencies on a number of parameters. Included in these parameters are edge and freestream Mach numbers, bluntness ratio, cone angle, enthalpy ratio, and mass addition effects. This is not the case in existing turbulent correlations. Both Bulmer<sup>14</sup> and Cassanto<sup>15</sup> have constructed turbulent base pressure correlations using only the edge Mach number  $M_e$  and the base-to-edge pressure ratio  $P_b/P_e$ . The

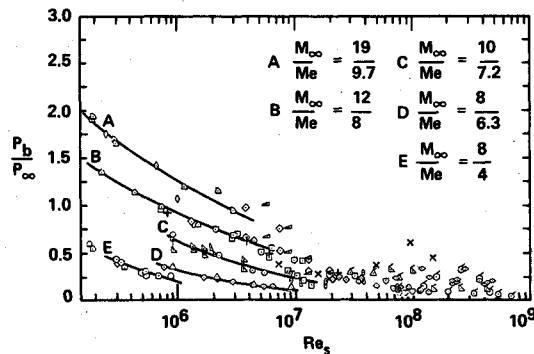


Fig. 5 Data presentation on turbulent coordinates.

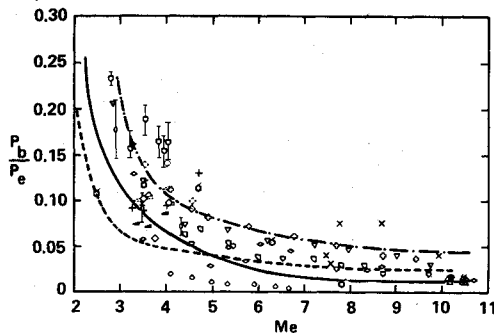


Fig. 6 Turbulent correlations of Bulmer and Cassanto.

success of such straightforward correlations in turbulent flow, when complex correlations were required in laminar flow, points out the different nature of the two regimes.

As a graphic illustration, Fig. 5 displays all of the laminar and turbulent data on the turbulent coordinates of this work. The strong dependencies on Mach number and bluntness ratio in the laminar regime are evident, as is the decay of those dependencies with increasing Reynolds number. The Reynolds number of turbulence onset is different for different vehicles, but it occurs near  $Re_s = 10^7$  for most of these vehicles. Figure 5 illustrates that this is also the region where the bluntness and Mach number effects have damped down. At still higher Reynolds numbers, the Mach number and bluntness effects are even less noticeable. This is true even though the range of these parameters actually is greater in the high Reynolds number turbulent regime than in the lower Reynolds number laminar regime.

The turbulent correlations of Bulmer and Cassanto are shown in Fig. 6. Note that Cassanto chose to model the base

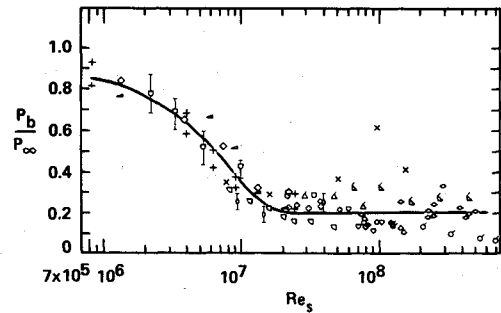


Fig. 7 Turbulent base pressure correlation.

pressure using a two-curve correlation, with the different curves representing different bluntness regimes. His distinguishing value of bluntness was updated recently from the original  $R_N/R_b = 0.1$  to  $R_N/R_b = 0.25$ . This two-level format has the unfortunate side effect of making numerical computations difficult near the changeover bluntness ratio.

The discrepancy between the Bulmer and Cassanto correlations is not due to a subjective selection of different curve fits of the same data, but rather to the use of a different data base in each case. Because of the limited nature of each data base and the apparent scatter in their coordinates, the range of applicability of each of these correlations is limited to vehicles having geometries, flight conditions, and materials properties similar to those of its data base. In order to estimate the intrinsic scatter in these coordinates, additional data containing a greater range of bluntness ratio, Mach number, and material properties were collected. These additional data, along with a sampling of the Bulmer and Cassanto data, are displayed in Fig. 6. The computation of edge conditions for these data included ablation effects. For these data,  $M_\infty$  ranged from 2 to 23. It is apparent that the different sets of data do not collapse to a single line in these coordinates but segregate according to the particular vehicle.

An alternative correlation similar to those of Bulmer and Cassanto in its basic simplicity is a plot of  $P_b/P_\infty$  vs  $Re_s$ . This provided an ordering, not a collapsing, in the laminar case of the data. In the turbulent case, however, the majority of the data do collapse in these coordinates, as seen in Fig. 7. It is important to note that in this correlation the base pressure is referenced to the freestream static pressure  $P_\infty$  and not to the edge pressure. This results in only the abscissa ( $Re_s$ ) being dependent on the various geometry, flight, and material properties, and not both the abscissa and ordinate as in the Cassanto-Bulmer correlations. Furthermore, the base pressure ratio is seen to be independent of Reynolds number for  $Re_s \geq 10^7$  when these data are considered as a group. This

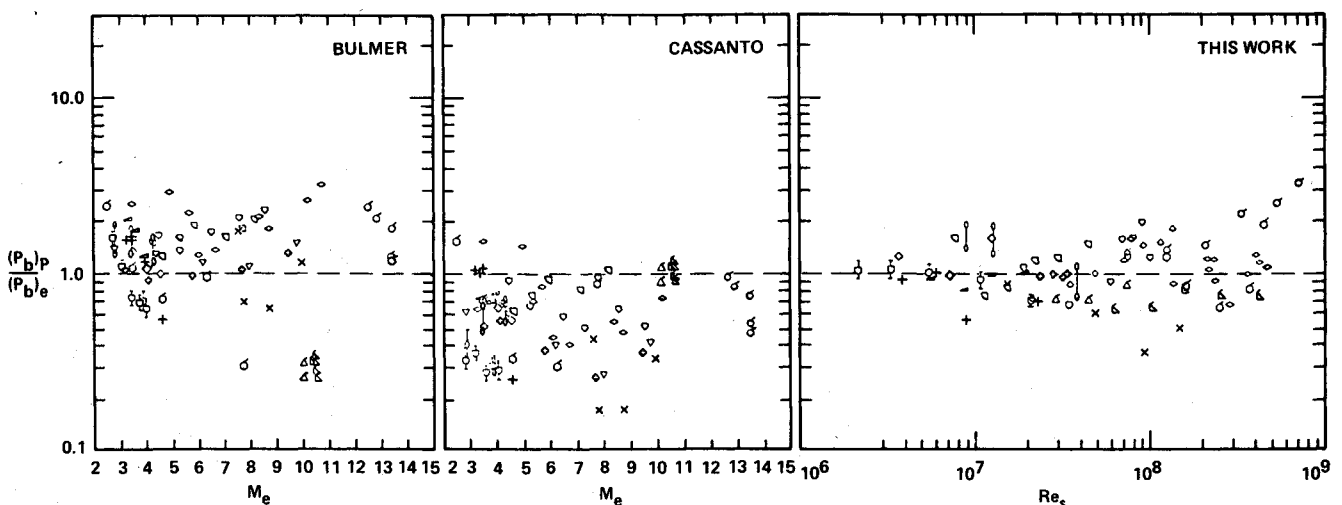


Fig. 8 Comparison of the predicted and experimental turbulent base pressures.

results in the somewhat surprising conclusion that the base pressure is a function only of altitude if  $Re_s \geq 10^7$ . Further study is required in this area to determine the significance of this trend and for which vehicles it applies. For any particular vehicle, there is a tendency for the base pressure ratio to decrease with altitude even on the "constant" portion of the curve. This effect has not been clearly identified yet with any particular variable, although it may be due to a Mach number effect or simply to the increase of  $P_\infty$  with decreasing altitude. The identification of such parameters is an area of consideration for future work.

A comparison of this new correlation to those of Bulmer and Cassanto, using the same format as in the laminar case, is shown in Fig. 8. The correlation of this work provides a modest improvement in the scatter over both the Bulmer and Cassanto correlations. In addition, it is in an analytically direct form and is adaptable readily to numerical analysis.

For all vehicles other than vehicle 7, there are only small circumferential gradients in  $M_\infty$ ,  $Re_s$ , and  $P_e$  at the edge of the boundary layer near the end of the vehicle. For vehicle 7, the geometrical and trim effects induce a substantial gradient in these edge conditions. This results in there being an entire range of edge conditions from which a particular set must be selected for use in the correlations. It is apparent from Figs. 6 and 7 that over a wide range of Reynolds and Mach numbers the correlations of Bulmer and Cassanto are nearly independent of edge Mach number, whereas the correlation of this work is independent of Reynolds number. Both the Cassanto and Bulmer correlations are, however, still strongly dependent on edge pressure. A change in the meridian at which the edge conditions are evaluated will then affect the level of the pressure ratio  $P_b/P_e$  significantly (Bulmer-Cassanto coordinates), but not the level of  $P_b/P_\infty$  (the coordinates of this work). This results in a sensitivity of the prediction accuracy to the particular meridian at which the edge conditions are evaluated in the Bulmer-Cassanto coordinates. Such a sensitivity is not seen in the correlation of the work for  $Re_s \geq 10^7$ . This effect is demonstrated in Figs. 9 and 10, where the same vehicle 7 base pressure data are

reduced with edge conditions from the windward and the side meridians. Note that there is nearly a factor of 7 difference in agreement using the same base pressure data between the windward and side meridians for the Bulmer-Cassanto coordinates; although there is little difference using the coordinates of this work, whereas this particular result is influenced by where the data fall on the respective curves, it does point out the sensitivity of base pressure estimates to the particular meridian at which the edge conditions are evaluated.

## Conclusions

### Laminar

The correlation of laminar flow base pressure considered in this paper has identified numerous geometric and flow parameters as influencing the base pressure. This complex dependence occurs both for correlations derived using strictly empirical techniques and for those derived using groupings of parameters suggested by analytic analyses. The particular parameters in each case are different. The selection of such different parameters does not appear to affect the data scatter significantly for the data taken as a group. The expected uncertainty in a prediction of base pressure using one of these correlations can be estimated from the magnitude of the scatter in data. It is apparent from this analysis that an uncertainty of  $\pm 50\%$  would not be unreasonable.

### Turbulent

In the turbulent regime, some interesting trends have been noted. Among these are the weak dependence of base pressure on edge Mach number, vehicle geometry, and freestream conditions  $M_\infty \geq 2$ . The complex groupings of parameters required in laminar flow no longer are required. Instead, coordinates involving only one parameter each appear to be sufficient. Several comparisons between the turbulent correlations have been noted. Among these are that the data scatter in the Bulmer-Cassanto coordinates is principally a vehicle-to-vehicle variation. Hence, a more accurate prediction of base pressure for a single type of vehicle is possible in these coordinates when a previously measured history of the particular vehicle of interest is known. For the data considered as a whole, the coordinates of this work provide a modest improvement.

It also has been noted that, for nonsymmetric vehicles or vehicles flying at angle of attack, the significant circumferential gradients in boundary-layer edge properties complicate the application of these correlations. For the limited amount of angle-of-attack data available, it appears that use of the boundary-layer properties on the side meridian results in nominal agreement with the flight data. The expected uncertainty in a prediction of base pressure using one of these correlations appears to be slightly greater than for the laminar case.

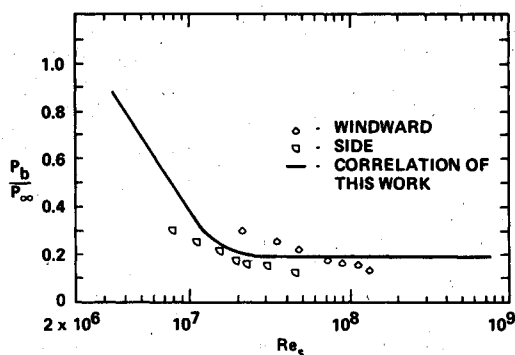


Fig. 9 Effects of angle of attack on vehicle 7 base pressure predictions.

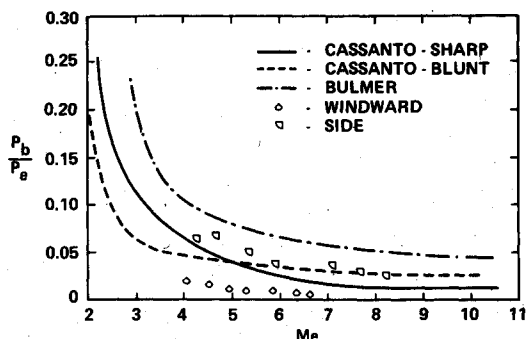


Fig. 10 Effects of angle of attack on vehicle 7 base pressure predictions.

## References

- Lees, L., "Hypersonic Wakes and Trails," *AIAA Journal*, Vol. 2, March 1964, pp. 417-428.
- Ohrenberger, J.T. and Baum, E., "Laminar Near Wake Solutions Under Atmospheric Entry Conditions," *AIAA Paper 72-116*, San Diego, Calif., 1972.
- Martellucci, A., "Laminar Base Pressure Correlations," General Electric Co., Philadelphia, Pa., GE-RESO ATC-DM-67-13, March 1967.
- Studerus, C.J. and Dienna, E.A., "Viscous Interaction Zero Angle of Attack Drag (VIZAAD) Program," General Electric Co., Philadelphia, Pa., GE TIS-64SD292, Nov. 1964.
- Bulmer, B.M., "Correlation of Re-Entry Base Pressure in Laminar Hypersonic Flow," Sandia Labs, SLA-74-169, Aug. 1974.
- Hochrein, G.J., "A Procedure for Computing Aerodynamic Heating on Sphere Cones - Program BLUNTY," Sandia Labs., SC-DR-69-449, Nov. 1969.
- Cassanto, J.M., "Base Pressure Results at Mach 19 from AEDC Tunnel F in Support of the GE/AEDC Base Pressure Program,"

General Electric Co., Philadelphia, Pa., GE-MSD-ATDM-67-04, Feb. 1967.

<sup>8</sup>Rie, H., "The GE-RESO Equilibrium Non-Similar Boundary Layer Program (ENSBL)," General Electric Co., Philadelphia, Pa., GE-TIS-71SD212, Feb. 1971.

<sup>9</sup>"Equations, Tables, and Charts for Compressible Flow," NACA TR-1135, 1953.

<sup>10</sup>Whitfield, J.D., "Critical Discussion of Experiments on Support Interference of Supersonic Speeds," Arnold Engineering Development Center, AAFS, Tenn, AEDC-TN-58-30, Aug. 1958.

<sup>11</sup>deKrasinski, J.S., "A Study of Axially Symmetrical Base Flow Behind Bodies of Revolution at Supersonic Speeds," *AGARD Conference Proceedings*, May 1966.

<sup>12</sup>Cassanto, J.M., "A Semi-Empirical Technique for Approximating the Base Pressure of Sphere-Cone Configurations in Laminar Flow at Hypersonic Mach Numbers," General Electric Co., Philadelphia, Pa., GE-RESO-ATFM-67-06, Feb. 27, 1967.

<sup>13</sup>Reeves, B.L. and Buss, H.M., "Theory of the Laminar Near Wake of Axisymmetric Slender Bodies in Hypersonic Flow," Avco, AVMSD-0122-69-RR, Feb. 1969.

<sup>14</sup>Bulmer, B.M., "Flight Test Base Pressure Measurements in Turbulent Flow," Sandia Corp., Rept. 76-0267, June 1976.

<sup>15</sup>Cassanto, J.M. and Storer, E.M., "A Revised Technique for Predicting the Base Pressure of Sphere-Cone Configurations in Turbulent Flow Including Mass Addition Effects," General Electric Co., Philadelphia, Pa., GE-RESO-ALFM-68-41, Oct. 1968.

<sup>16</sup>"Test Facilities Handbook," 9th ed., Arnold Engineering Development Center, July 1971.

<sup>17</sup>Ward, L.K. and Choate, R.H., "A Model Drop Technique for Free Flight Measurements in Hypersonic Wind Tunnels using Telemetry," Arnold Engineering Development Center, AAFS, Tenn, AEDC-TR-66-77, May 1966.

<sup>18</sup>Softley, E.J. and Graber, B.C., "Techniques for Low Level Pressure and Heat Transfer Measurements and their Application to Base Flows," General Electric Co., Philadelphia, Pa., GE-SSL-TIS-R67SD2, Feb. 1967.

<sup>19</sup>Cassanto, J.M., "Base Pressure Results on 10° Sharp and Blunt Cones at Mach Numbers 2.0 and 4.0 in Support of the GE/AEDC Base Pressure Program," General Electric Co., Philadelphia, Pa., GE-MSD-ATDM-66-20, Oct. 1966.

<sup>20</sup>Martellucci, A., Ranlet, J., Schlesinger, A.J., and Garberoglio, J., "Experimental Study of Near Wakes—Data Presentation," General Applied Science Labs, GASL TR641, Dec. 1966.

## *From the AIAA Progress in Astronautics and Aeronautics Series . . .*

### **GUIDANCE AND CONTROL—v. 8**

*Edited by Robert E. Roberson, Consultant, and James S. Farrior, Lockheed Missiles and Space Company.*

The twenty-nine papers in this volume on space guidance and attitude control cover ascent, space operations, descent, inertial navigation, inertial components, optical navigation, adaptive systems, and attitude control.

Guidance studies cover launch-time variations, booster injection, station keeping, trajectory analysis and prediction, with various types of perturbation and consequent propellant requirements. Lunar missions are analyzed as a type of four-body problem, and a soft landing terminal guidance system is proposed.

Inertial guidance systems are analyzed and proposed, emphasizing error detection and correction routines as applied to servomechanism theory, recognizing the fundamental limitations of inertial systems. Several inertial system components are analyzed, mainly miniaturized high-precision gyros of several types.

Optical navigation systems considered include infrared, optical Doppler systems, and optical frequency shift detection. Adaptive control systems anticipate future projects and engine-out operational capability. Various satellite attitude control systems are treated, and a number of stabilization systems are considered.

670 pp., 6 x 9, illus. \$16.50 Mem. & List

TO ORDER WRITE: Publications Dept., AIAA, 1290 Avenue of the Americas, New York, N. Y. 10019